

Droplet Breakup Regime in a Cross-Junction Device with Lateral Obstacles

Tawfiq Chekifi^{1,*}

Abstract: Numerical simulation using Ansys Fluent code is performed, to investigate droplet generation in cross-junction based VOF method. Droplets of water are generated by the shear stress applied by continuous phase (oil), two configurations of cross-junction are suggested; the first is a simple model no modification is performed at the outer channel, while the second model is characterized by a lateral obstacle. we study the effect of velocity ratio, viscous parameter, interfacial tension, flow condition on droplet size and frequency, the effect of lateral obstacles on droplets generation is also focused and analysed. The numerical simulations showed that the velocity ratio and interfacial tension play a significant role in determining the droplet breakup and non-breakup. On the other side, the increase of flow rate ratio can be effectively used to decrease the droplet size. In addition, droplets produced in cross-junction with lateral obstacles are generally found to be larger than that produced with the first model. Moreover, the frequency of droplet production was increasing by increasing of flow rate ratio. The numerical results show very good agreements with previous numerical and experimental works for the growth of droplet breakup, size and frequency.

Keywords: Water droplet, cross-junction, CFD, VOF, microchannel.

1 Introduction

Year on Year, droplet based microfluidic is advancing rapidly in several application such as biomedicine [Mazutis and Griffiths (2012)], pharmaceuticals [Nabavi, Vladislavljević, Gu et al. (2015)], agriculture [Jia, Li, Qiu et al. (2008)], lab on chip [Carreras, Elani, Law et al. (2015)]. In this field, two main subject attracting researchers from several domains: Firstly, droplet generation; in this axis, researchers focused on many parameters effecting droplet formation such as, droplets size, frequency, shape, fluids proprieties, ...etc. several concepts were proposed to generate the droplet (T-junction, cross-junction, flow focusing, co-flow). In these configurations the droplet phase is forced by the continuous (oil) phase which leads to rupture the head of dispersed phase to form a small droplet, this process is characterized by the capillary number. The second subject is droplet manipulation; this stage is usually the second step after the droplet formation. Computational fluid dynamics (CFD) is a useful tool in fluid mechanic application, it provides many information on flow dynamic details (pressures, velocities...etc.) that are perhaps difficult to get them experimentally. In recent years, several techniques were used for interface tracking

¹ Research Center in Industrial Technologies CRTI, P.O. Box 64, Cheraga Algiers, Algeria.

* Corresponding Author: Tawfiq Chekifi. Email: t.chekifi@crti.dz; chekifi.tawfiq@gmail.com.

[Chekifi, Dennai and Khelfaoui (2015)]. According to the tracking form, two kinds of methods are categorized: explicit and implicit tracking methods. The explicit tracking regroups: boundary integral method, immersed interface method and front tracking method, whereas the Implicit one regroups: level-set method and phase-field method. Different numerical works have been investigated the droplet formation and its dynamics inside microchannel system. Umbanhowar et al. [Umbanhowar, Prasad and Weitz (2000)] used the VOF method with Fluent simulation, to investigate the creation of droplets and bubbles in trapped channel system. Suryo et al. [Suryo and Basaran (2006)] numerically explored the droplet generation from a capillary tube, incompressible Newtonian fluid, finite element method and an adaptive finite difference method was performed, the droplet shapes, fluid velocities and pressures were studied, it was shown that increasing of the flow rate ratio decreases the volume of droplets. Lee et al. [Lee, Lee and Son (2013)] performed numerical simulation based VOF method using the commercial code FLUENT, droplet merging by the use of an obstacle in the outer microchannel was presented, where diamond-shaped configuration obstacle was found effective for droplet breakup, Using the commercial software FLUENT, Hong et al. [Hong and Wang (2007)] studied the flow rate effect on droplet formation in a flow focusing microfluidic device. Four droplet design was distinguished; monodisperse beads with little bead satellite, Polydisperse drops, laminar streams are framed and just monodisperse droplets. also, beads estimate was observed to be roughly free of or firmly subject to the stream rate proportion. Also Wu et al. [Wu, Tsutahara, Kim et al. (2008)] proposed an improved immiscible LBM show for bead development in a cross-intersection microchannel, by combining CFS model and immiscible LBGK model, the author achieved the correct interfacial tension. On the author side, the influence of capillary number on droplet size has been focused, where several profiles of droplet shape has been identified as function of Ca, Moreover Liu et al. [Liu and Zhang (2011)] investigated droplet formation with cross-junctions design, as a result of connection between two immiscible fluids, three different flow regimes were identified to be dependent on the capillary number and the flow conditions of both phases. In addition, the author focused the influence of dimensionless geometrical, capillary number, and flow rate ratio on the droplet generation.

In cross-junction configuration, the dispersed phase channel is located between two channels of continuous phase, consequently, uniform shear stress is surrounded the dispersed phase. The competition between the shear forces and surface tension, as a result, the thread head becomes unstable and produces droplet. Although many previous work on droplet production by cross-junction and flow-focusing concept have been carried out, either numerical or experimental work, a fundamental understanding of the droplet breakup and non-breakup, that represent the impact of the geometry of the gadgets and recreation of these marvel, utilizing VOF technique based CFD familiar are as yet absent. This method has been proved to be a functional method to simulate immiscible fluids flows [Lee, Lee and Son (2013)]. In the present paper, we investigate the droplet generation using cross-junction channel device for low Reynolds and Capillary numbers. We define the droplet magnitude, it's formation frequency with different changes of flow conditions as well as geometrical configuration. In this work, droplet shape and magnitude depend on velocities ratio and viscosities ratio. In addition, droplet flow regime (breakup and non-breakup) is found to be related to interfacial tension. The numerical results have been viewed as a comparison with available numerical

and experimental results data for validation.

2 Model description and numerical method

The proposed cross-junction configuration is composed of three inlet channels, two side channel includes oil and middle one contains water, and outlet channel. The novelty in this configuration is the small wall considered as a lateral obstacle on the outer channel (called also a chicane), this modification is assumed to effect the droplet breakup regime and its generation frequency.

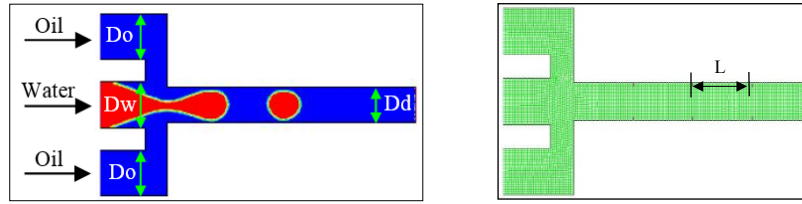


Figure 1: Schematic description of the cross-junction configuration: $D_w=D_o=1$ mm, $D_d=0.8$ mm, $L=1.25$ mm shown in right model $L_{wall}=0.1$ mm

In this numerical study, the volume of fluid technique is utilized to examine the droplet generation by cross-junction device, in this method the volume fraction of one fluid phase (denoted as C) is considered to characterize the interface. Moreover, the phase averaging is used to determine in each cell the volume of dispersed phase and continuous. For that the variable, α , is defined as:

- $\alpha=0$ when the cell is 100% loaded up with water.
- $\alpha=1$ when the cell is 100% loaded up with oil.
- $0<\alpha<1$ when the cell contains an interface between the two phases.

The viscosity μ and the density ρ , for both phases (oil and water) are estimated using a linear dependence:

$$\rho=\rho_w \alpha+\rho_o (1-\alpha) \quad (1)$$

$$\mu=\mu_w \alpha+\mu_o (1-\alpha) \quad (2)$$

The governing equations describing both phases motion are the mass conservation and the momentum equation [Hirt and Nicholas (1981)]:

$$\partial_t c + \vec{u} \nabla c = 0 \quad (3)$$

where the velocity is given by u . In addition, a single momentum equation is used for two-phase-fluid described by Kleefsman et al. [Kleefsman, Fekken, Veldman et al. (2005)]:

$$\frac{\partial}{\partial t}(\rho \vec{u}) + \nabla \cdot (\rho \vec{u} \vec{u}) + \nabla \vec{u} \cdot \nabla [\mu] = -\nabla P - F_{sur} \quad (4)$$

where $F = \sigma \kappa (\mathbf{x}) \mathbf{n}$, κ is the surface tension force and \mathbf{n} is a unit vector normal to the interface. σ is the surface tension coefficient [Reitzle, Kieffer-Roth, Garcke et al. (2017)]

$$F_{sur} = \sigma \frac{2\rho \kappa_1 \nabla \alpha_1}{\rho_1 + \rho_2} \quad (5)$$

κ_1 being the interface curvature computed as [Lee, Walker and Anna (2009)]:

$$\kappa_1 = -\nabla \cdot (\nabla \alpha_1 / |\nabla \alpha_1|) \quad (6)$$

In the VOF method, the Courant number is defined as:

$$Co = \frac{\Delta t}{\Delta x / V_{\text{fluid}}} \quad (7)$$

We set the global maximum Courant number to 0.25 to accelerate the convergence rate while keeping up the precision of count. Near the interface, geometric reconstruction scheme is utilized to precise interface. The initial phase in reconstruction scheme, is ascertaining the situation of the straight interface with respect to the focal point of each in part filled cell. The second phase is figuring the advecting measure of liquid through each face. The third step is computing the volume part in every cell. The two models of geometry (without and with chicane) and meshes were produced utilizing Gambit software. A quadratic mesh was utilized on all geometry that the estimations of surface tension special effects are more precise compared to a tetrahedral and triangular mesh. So as to enhance the resolution of the droplet breakup zone. The velocity inlet in both phase inlets used while atmospheric pressure (100000 bar) was applied in the output as a boundary conditions, moreover no-slip boundary conditions at all the walls is defined. furthermore, the second-order scheme was used for discretization of the momentum equation. The SIMPLE and PRESTO! were taken as both the pressure-velocity coupling scheme and the pressure discretization scheme. The geometric reconstruction scheme was utilized for volume fraction calculation. The convergence was achieved for (10^{-5}) of time steps to produce a database. The residual was 10^{-3} for all continuity components.

The fundamental relating dimensionless number used to describe the droplet formation is the Capillary number which compares the competition between surface tension forces and viscous forces. $Ca = v\mu/\sigma$, where the viscosity of oil is typically used, creating constant droplets is the main phase of realizing droplet. Expending pressure as dynamic force to create droplet is one of the fastest and frequently used methods.

3 Volume of fluid model validation

Recently, CFD codes as Ansys fluent were widely used for droplet breakup simulation. In this subsection, the volume of fluid method is tested for droplet formation and compared to previous available works, the results are presented in the following table.

Significant data are existing in the literature for the droplet formation, the previous works have been performed on cross-junction by either numerical or experimental approaches as shown in above table, the same fluids (water and oil) are used in this test, while the geometry dimension, the viscosity ratio and flow rate ratio are different which is normal to check a qualitative comparison and validation. a comparison of droplet flow regime with Shi et al. [Shi, Tang and Xia (2014)] shows a good covenant in term of droplet size and diameter. In addition, increasing of flow rate ratio leads to increasing of droplet diameter. The model was also legalized by comparing the obtained results beside a wide variety of experimental results in the form of the sequential photographs presented by Shi et al. [Shi, Tang and Xia (2014)]. After the above evaluations and examination, all the quantitative and qualitative numerical results are in respectable agreement with VOF method results. Therefore, the methodology in the present numerical work is reliable and efficient for the

research of droplet flow inside corss-junction concept. Consequently, further examinations can be approved based on the method.

Table 1: Droplets generation comparison

Ref.	Geometry/size	Fluids	(μ_d/μ_c)	(Q_d/Q_c)	Droplet diameter
[Shi, Tang and Xia (2014)] (LBM method)	$W_o=W_w=20 \mu\text{m}$	Water in oil	1/4	0.11	70 μm
	$W_d=12 \mu\text{m}$			0.3	95.8 μm
	(80×340 μm)			0.5	155 μm
[Liu and Zhang (2011)] (LBM method)	$W_d=200 \mu\text{m}, h=100 \mu\text{m}$	Water in oil	1/6	0.1	170 μm
	$W_c=100 \mu\text{m},$			0.5	220 μm
	(2290×610×110 μm)			1	340 μm
[Chekifi (2018)] (VOF method)	$W_o=W_w=1 \text{mm}$	Water in oil	1/3	0.1	0.3 mm
	$W_d=0.8 \text{mm}$			0.14	0.4 mm
	(4×7 mm)			0.2	0.61 mm
[Wu, Tsutahara, Kim et al. (2008)] experiments	$W_d=200 \mu\text{m}, h=100 \mu\text{m}$	Water in oil	$0.74 \times 10^{-2}/$ 4.41×10^{-2}	0.16	0.275 mm
	$W_c=100 \mu\text{m}$			0.33	0.3 mm
				1	0.41 mm

4 Results and discussion

In this subsection, we examine the droplet breakup using cross-junction channel with VOF method, the effect of fluid proprieties, flow conditions and geometry are investigated and compared with available data3 as follow: Firstly, we check the droplet deformation behavior using Taylor deformation model, secondly, we investigate the effect of velocity ratio and interfacial tension on breakup and non-breakup, then we examine the flow rate ratio on droplets size in Section 4.4, finally, the droplet generation frequency is investigated and presented in Section 4.5

4.1 Taylor deformation under shear flow

Taylor deformation is frequently used to examine droplet deformation manners in a binary model. A droplet is placed in the middle of two shearing plates which are moving at the opposite orders to obtain a linear shear in the Stokes regime. For a droplet in the Stokes regime with small capillary number, the breakup follows a theoretical relation as [Roths Marth, Honerkamp et al. (2002)]:

$$\text{Deformation} = f\left(\frac{\eta_d}{\eta_c}\right) \cdot Ca = 0.25 \cdot Ca \tag{8}$$

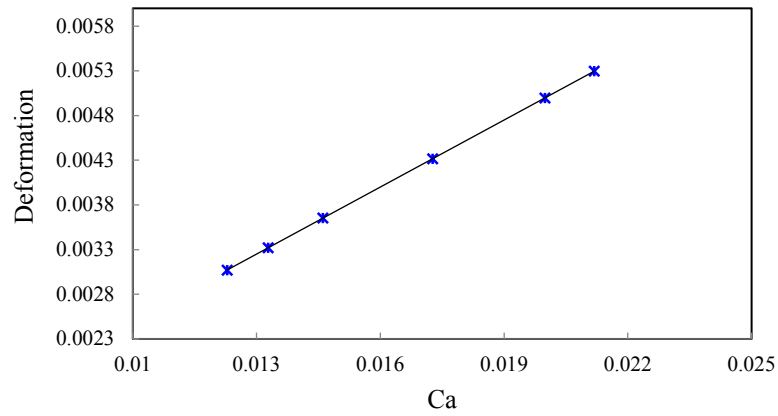


Figure 2: Variation of droplet deformation as function of capillary number

Fig. 2 presents the variation of droplet deformation at six capillary number values, with the increasing capillary number; the deformation of the droplet becomes more serious. In this illustration, the linear relationship of $Deformation=0.25.Ca$ between the deformation and capillary number is obtained based on the present simulation results. With the increasing of the capillary number, the droplet is generated when the capillary number exceeds a critical value. The present profile agrees well with the ones presented in Shi et al. [Shi, Tang and Xia (2014)]. It indicates that the droplet deformation is in elasticity mode.

4.2 Effect of velocity ratio

Droplet breakup is typically affected by the flow dynamics of both the continuous and the dispersed phase, Jia et al. [Jia, Li, Qiu et al. (2008)] presented a lattice Boltzmann simulations of droplet breakup using a cross-junction configuration channel. In this subsection, we consider the effects of velocity ratio on flow pattern with fixed viscosity ratio and interfacial tension of both phases. Numerical simulations are performed for a range of flow velocity to identify the droplet breakup interval, the values of velocity are taken referring to our previous work [Chekifi (2018)].

In Fig. 3, the densities of the continuous (oil) and dispersed phase (water) are assumed to be constant ($\rho_w=998.2 \text{ kg/m}^3$ $\rho_o=830 \text{ kg/m}^3$).

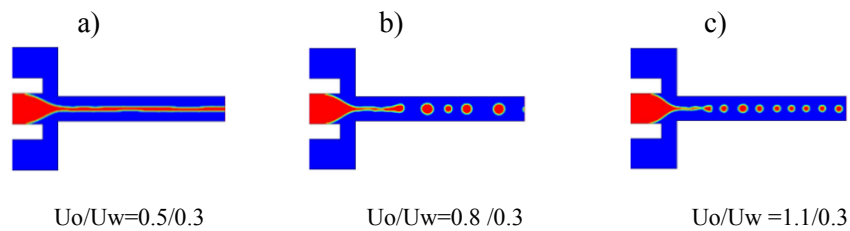


Figure 3: The effects of flow rate ratio and viscosity ratio on droplet diameter with a fixed interfacial tension $\sigma=1.5 \text{ N/m}$

Three flow regimes are presented as function of velocity ratio of continuous phase to dispersed phase; parallel phases flow (or continuous flow) (Fig. 3(a)), in this regime no droplets breakup is occurred, where both phases are flowing together inside the outer channel, in this case the shear flow forces cannot overcome the interfacial forces leading to a continuous flow stream. Increasing of flow velocity ratio Figs. 3(b) and 3(c), makes the shear flow forces much bigger than the interfacial forces, which creates an instability of the continuous phase (oil) stream and facilitates breaking of the droplets. Nevertheless, droplets size is decreasing as the viscosity ratio U_o/U_w increases, due to the important difference between shear flow and interfacial tension forces as well as [Gupta, Murshed and Kumar (2009)] observed in his experiment work. On the other hand, we observe that the produced droplets are monodispersed when the droplet is produced in or close to the junction. This kind of droplet breakup is usually called dripping mode, In addition, droplets were not generated at very low velocity, since the oil phase invade the dispersed c due to the very low flow rate of the later, which was also associated with the high viscosity. Another motivating result can be assumed is that the droplet size is directly dependent on the viscosity ratio of both fluids.

4.3 Interfacial tension effect

The interfacial tension plays a significant rule on the flow of two phases especially for liquid-liquid and liquid-gas, the surface tension forces are necessary in determining the dynamics of droplets, while gravitational forces are generally less important, as reported in many previous works [Zhu, Kong, Lei et al. (2016); Costa, Gomes and Cunha (2017)]. In this subsection, the effect of interfacial tension on the droplet flow patterns is focused, however two parameters are tested; for the collection A; water is set up to 0.3 Pa and oil inlet was set up to 0.7 Pa, whereas in the collection B; water is applied in 0.1 Pa and oil in 0.6, the pressure at output system was the atmospheric pressure for both collections, the values of interfacial tension are taken referring to our previous work in Chekifi et al. [Chekifi, Dennai and Khelifaoui (2015)].

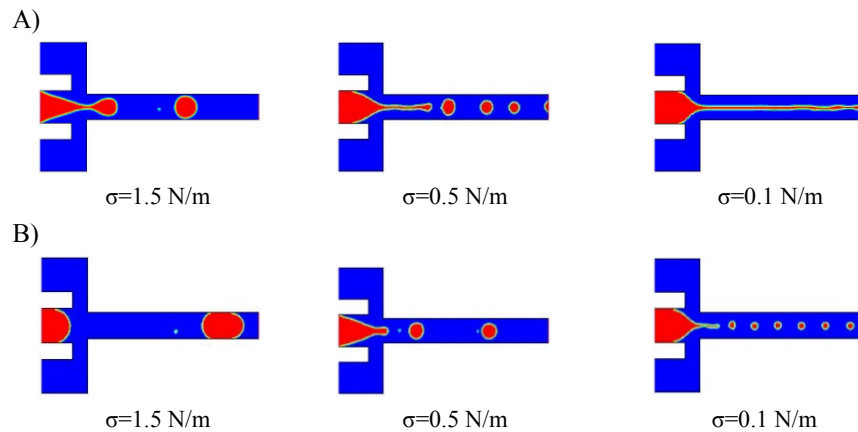


Figure 4: Droplet formation regime occurring in the downstream as function of interfacial tension between water and oil

The Fig. 4 shows the influence of interfacial tension on the droplet patterns for different capillary number, we use water as the dispersed phase and oil as the continuous phase, and observe flow regime which depends on the surface tension coefficient. The densities of the continuous and dispersed phase are assumed respectively $\rho_w=998.2 \text{ m}^3/\text{kg}$ and $\rho_o=830 \text{ m}^3/\text{kg}$. It is shown in Fig. 4 that for Capillary numbers. In both groups (A and B): decreasing of interfacial tension from 1.5 N/m to 0.1 N/m from leads to the transformation of droplet breakup pattern from dripping to jetting regime, with a “stable” droplet formation regime in a microchannel, thread regime of dispersed phase is clearly observed (Fig. 4(A): $\sigma=1.5 \text{ N/m}$), as we increase. On the other hand, in Fig. 4(A), $\sigma=0.1 \text{ N/m}$ droplet breakup has not been achieved due to the high pressure applied on oil in this test $Po=0.7 \text{ Pa}$. for higher surface tension $\sigma=1.5 \text{ N/m}$, droplet are formed with high dispersion due to the squeezing mechanism, from the Fig. 4, the interfacial tension influences droplet formation regime and droplet volume, this result was also obtained in our numerical simulation published previously using flow focusing configuration [Chekifi, Dennai and Khelifaoui (2015)].

4.4 Flow rate and geometry effects

Droplets are generated at the cross-junction by shear stress applied by oil on water, however in this subsection, the effect of lateral chicane on droplet formation has been studied, for a range of Capillary numbers, by varying the flow rate ratio, as well as viscosity ratio of both fluids inlets. While the other parameters are kept fixed. However, the flow rate ratio has been selected based on reported values for which monodisperse droplet formation was reported in the literature [Gupta, Matharoo and Makkar (2014)]. The same geometry as one taken for grid independence test is used. The parameters which have been varied are viscosity ratio, flow rate ratio and the outer channel configuration. The next flow factors are held stable in this study: flow rate ratio and viscosity ratio. Ca has been chosen to be much less than 1 so as to be confined to the squeezing regime of droplet formation

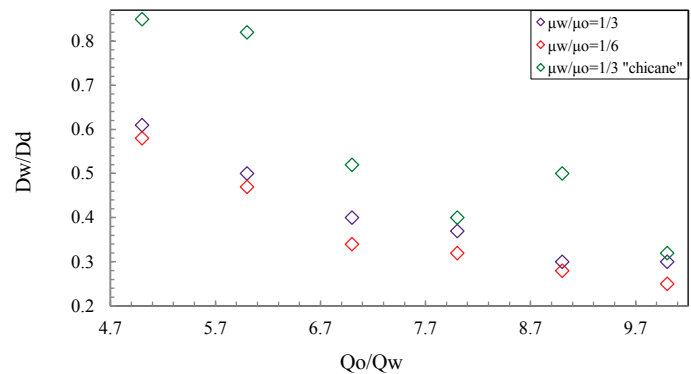


Figure 5: Normalized length of droplets vs. flow rate ratio of two inlets at a fixed $Ca=0.006$

The droplet size (D_w) normalized to the characteristic length of the water channel (D_d) versus the flow-rate ratio for different values of viscosity ratio μ_w/μ_o is shown in Fig. 5. The Fig. 5 shows droplet breakup development in cross junction concept, before droplet get produced, the procedure takes place in three stages, in which the water thread develops

to take the conical form, at that moment the shear stress applied by oil enforces the water head, the later breaks up to provide birth of droplet. It is clearly observed that the droplet dimension becomes bigger when the flow rate ratio is increasing with a fixed flow rate of oil. From Fig. 5, we can appreciate that the droplet diameter declines as the viscosity ratio of water to oil decreases, while growing the viscosity of oil leads to increase the inertia force applied on the water fluid, which allows to surpass the surface tension potency and breaks up the dispersed fluid thread quicker, leading to create a minor droplet size. Consequently, the small viscosity ratio μ_w/μ_o and high-dispersed flow rate will force the position of droplet detachment point to move further to the downstream. On the other side, declining the viscous stress of oil fluid $\mu_w/\mu_o=1/3$ (Fig. 4) allows to nearly decrease the shear forces, results in slower break of the water thread; accordingly bigger droplet is shaped into the external channel. Compared with geometry effect, our numerical simulation show that the modified channel (with lateral obstacle) has its advantages when the position of the droplet detachment point moves to the downstream at a higher viscosity and flow rate of the dispersed phase. Moreover, a motivating result can be assumed is that the droplet magnitude is a little dependent on the viscosity ratio of both phases.

4.5 Droplet formation frequency

The droplet generation frequency is very important parameter, for the applications of droplet in several fields, it allows identifying the number of droplets produced per second, the frequency is given by: $fr=1/\Delta t$; where Δt defines the time difference between two droplets. In this study, the satellite droplets are neglected, in term of frequency investigation. Using the simple cross-junction configuration (without lateral obstacles) presented previously, computations have been conducted to characterize the impact of the flow rate ratio, the viscosity ratio. simulations have been completed for $Re < 200$.

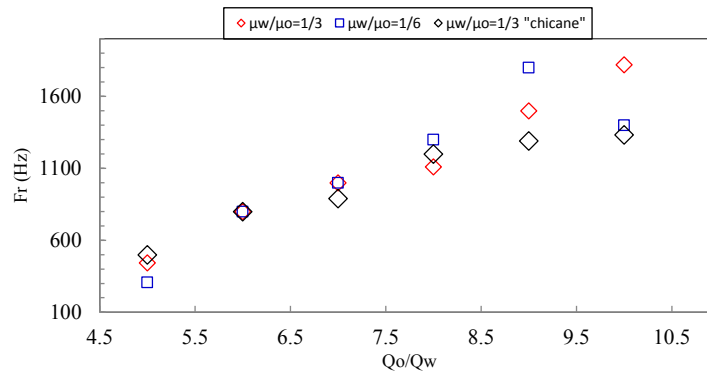


Figure 6: Droplet production frequency for both models as function of flow rate ratio and viscosity ratio; $\mu_w/\mu_o=1/3$, $\mu_w/\mu_o=1/6$

The viscosity ratio is defined as the ratio between the dynamic viscosity of the water fluid to that of oil. For this study, the surface tension was kept fixed, while the frequency has been identified using the volume fraction of water at the output of microsystem, As the flow rate ratio increases, the frequency was found to increase, due to the growth of shear stress applied by the oil and make the operation quicker. A slightly variation in frequency

of droplet production can be observed with variation of viscosity ratio and geometry models, Though, growing the flow velocity ratio in both cross-junction models conducts droplets to be formed with high frequency, whereas the droplet length was declining. This work also proves that the VOF model is an operational method to simulate the droplets production in corss-junction channel geometry.

5 Conclusion

Numerical simulation using the VOF method has been performed, to investigate the effect of flow parameters and geometry configuration, on droplet production by cross junction channel. However, water droplets are formed with the result of the shear stress applied on the dispersed phase by the continuous phase. The viscosity ratio and lateral small walls marginally influenced the droplet breakup, with low viscosity ratio ($\mu^*=1/6$) droplets were slightly larger than that obtained for high viscosity ratio ($\mu^*=1/3$). On the other side, the interfacial tension significantly affected the droplet formation patterns; dripping regime is identified for high interfacial tension (1.5 N/m), while the jetting regime was observed for low interfacial tension (0.5 N/m). Moreover, the frequency was also dependent on flow rate ratio and the geometry size. for the same geometry, it is also observed that the increasing of flow rate leads to the increasing of frequency leads while the droplet size decreases. The numerical results revealed that droplet breakup regime, frequency and size are mainly dependent on both lateral walls and principally the flow rate ratio. Finally, droplets generation frequency and size in the cross-junction channel can be controlled by changing the viscosity ratio, the velocity ratio as well as flow rate.

References

- Carreras, P.; Elani, Y.; Law, R. V.; Brooks, N. J.; Seddon, J. M. et al.** (2015): A microfluidic platform for size-dependent generation of droplet interface bilayer networks on rails. *Biomicrofluidics*, vol. 9, no. 6, 064121.
- Chekifi, T.** (2018): Computational study of droplet breakup in a trapped channel configuration using volume of fluid method. *Flow Measurement and Instrumentation*, vol. 59, no. 2018, pp. 118-125.
- Chekifi, T.; Dennai, B.; Khelifaoui, R.** (2015): Numerical simulation of droplet breakup, splitting and sorting in a microfluidic device. *Fluid Dynamics & Materials Processing*, vol. 11, no. 3, pp. 205-220.
- Costa, A. L. R.; Gomes, A.; Cunha, R. L.** (2017): Studies of droplets formation regime and actual flow rate of liquid-liquid flows in flow-focusing microfluidic devices. *Experimental Thermal and Fluid Science*, vol. 85, no. 2017, pp. 167-175.
- Gupta, A.; Matharoo, H. S.; Makkar, D.; Kumar, R.** (2014): Droplet formation via squeezing mechanism in a microfluidic flow-focusing device. *Computers & Fluids*, vol. 100, no. 2014, pp. 218-226.
- Gupta, A.; Murshed, S. M. S.; Kumar, R.** (2009): Droplet formation and stability of flows in a microfluidic T-junction. *Applied Physics Letters*, vol. 94, no. 16, 164107.
- Hirt, C. W.; Nichols, B. D.** (1981): Volume of fluid (VOF) method for the dynamics of free boundaries. *Journal of Computational Physics*, vol. 39, no. 1981, pp. 201-225.

- Hong, Y.; Wang, F.** (2007): Flow rate effect on droplet control in a co-flowing microfluidic device. *Microfluidics and Nanofluidics*, vol. 3, no. 3, pp. 341-346.
- Kleefsman, K.; Fekken, G.; Veldman, A.; Iwanowski, B.; Buchner, B.** (2005): A volume-of-fluid based simulation method for wave impact problems. *Journal of Computational Physics*, vol. 206, no. 1, pp. 363-393.
- Lee, J.; Lee, W.; Son, G.** (2013): Numerical study of droplet breakup and merging in a microfluidic channel. *Journal of Mechanical Science and Technology*, vol. 27, no. 6, pp. 1693-1699.
- Lee, W.; Walker, L. M.; Anna, S. L.** (2009): Role of geometry and fluid properties in droplet and thread formation processes in planar flow focusing. *Physics of Fluids*, vol. 21, no. 3, 032103.
- Liu, H.; Zhang, Y.** (2011): Droplet formation in microfluidic cross-junctions. *Physics of Fluids*, vol. 23, no. 8, 082101.
- Mazutis, L.; Griffiths, A. D.** (2012): Selective droplet coalescence using microfluidic systems. *Lab Chip*, vol. 12, no. 10, pp. 1800-1806.
- Nabavi, S. A.; Vladisavljević, G. T.; Gu, S.; Ekanem, E. E.** (2015): Double emulsion production in glass capillary microfluidic device: parametric investigation of droplet generation behaviour. *Chemical Engineering Science*, vol. 130, no. 2015, pp. 183-196.
- Reitzle, M.; Kieffer-Roth, C.; Garcke, H.; Weigand, B.** (2017): A volume-of-fluid method for three-dimensional hexagonal solidification processes. *Journal of Computational Physics*, vol. 339, no. 2, pp. 356-369.
- Roths, T.; Friedrich, C.; Marth, M.; Honerkamp, J.** (2002): Dynamics and rheology of the morphology of immiscible polymer blends-on modeling and simulation. *Rheol Acta*, vol. 41, no. 3, pp. 211-222.
- Shi, Y.; Tang, G. H.; Xia, H. H.** (2014): Lattice Boltzmann simulation of droplet formation in T-junction and flow focusing devices. *Computers & Fluids*, vol. 90, no. 2014, pp. 155-163.
- Suryo, R.; Basaran, O. A.** (2006). Tip streaming from a liquid drop forming from a tube in a co-flowing outer fluid. *Physics of Fluids*, vol. 18, no. 8, 082102.
- Umbanhowar, P.; Prasad, V.; Weitz, D.** (2000): Monodisperse emulsion generation via drop break off in a coflowing stream. *Langmuir*, vol. 16, no. 2, pp. 347-351.
- Jia, W. D.; Li, P. P.; Qiu, B. J.; Fu, X. X.; Xue, X. Y.** (2008): Experimental investigation of droplet diameter and velocity distributions in agricultural electrostatic sprays. *Transactions of the Chinese Society of Agricultural Engineering*, vol. 2008, no. 2
- Wu, L.; Tsutahara, M.; Kim, L. S.; Ha, M.** (2008): Three-dimensional lattice Boltzmann simulations of droplet formation in a cross-junction microchannel. *International Journal of Multiphase Flow*, vol. 34, no. 9, pp. 852-864.
- Zhu, P.; Kong, T.; Lei, L.; Tian, X.; Kang, Z. et al.** (2016): Droplet breakup in expansion-contraction microchannels. *Scientific Reports*, vol. 6, no. 1, pp. 21527.